2.2 kW Single-Mode Narrow-Linewidth Laser Delivery Through a Hollow-Core Fiber

M. A. Cooper[1,*], J. Wahlen[1], S. Yerolatsitis[1], J. E. Antonio-Lopez[1], D. Cruz Delgado[1], D. Parra[1], B. Tanner[2], O. Jones[2], I. Divliansky[1], A. Schülzgen[1], and R. Amezcua Correa[1,*]

[1] CREOL, The College of Optics and Photonics, University of Central Florida, 4304 Scorpius St, Orlando, FL 32816
[2] Coherent Corp, 3340 Parkland Ct, Traverse City, MI, 49686
[*] m.cooper@knights.ucf.edu
[*] r.amezcua@creol.ucf.edu

Compiled May 24, 2023

Antiresonant hollow-core fibers (AR-HCFs) have opened up exciting possibilities for high-energy and high-power laser delivery, thanks to their exceptionally low nonlinearities and high damage thresholds. While these fiber designs offer great potential for handling kilowatt-class powers, it is crucial to understand their fundamental limitations by investigating their performance at multi-kW power levels. Until now, efforts to deliver a narrow-linewidth single-mode laser at multi-kW power levels through a hollow core fiber have been unsuccessful. Here, we demonstrate the successful delivery of a record 2.2 kW laser power with a spectral linewidth of 84 GHz, centered at 1080 nm, while maintaining over 95% efficiency. This was achieved using a 6.25 m long AR-HCF with low-loss properties. Furthermore, we show power delivery of 1.7 kW with a spectral linewidth as narrow as 38 GHz. Our results could lead to a new generation of fiber-based laser beam delivery systems with applications in precision machining, nonlinear science, and directed energy.

http://dx.doi.org/10.1364/ao.XX.XXXXXX

In recent years, the delivery of high-power single-mode laser beams through hollow-core optical fibers has undergone substantial experimental advancements. These developments have been fueled by the potential application of this technology in key areas including precision manufacturing [1], ultrafast physics [2–5], telecommunications [6–9], and directed energy [10–12] to mention a few. In general, the goal of single-mode laser beam delivery fibers is to preserve the spectral and spatial features of the source at a remote point of interest. This is especially relevant in applications where beam focusing near the diffraction limit is required to achieve high precision and accuracy. Nevertheless, high-power transmission through solid core fibers at long lengths suffer from numerous deleterious phenomena due to intensity based non-linear effects such as the Kerr effect, stimulated Raman scattering (SRS), and stimulated Brillouin scattering (SBS) [13–15]. These effects impose significant constraints on the power levels that can be transmitted through a solid core optical fiber. In particular, high-power Ytterbium-doped (Yb-doped) single-mode narrow-linewidth fiber lasers are typically restricted by SBS, while SRS limits high-power broadband performance [10, 14].

The concept of photonic bandgap introduced the possibility of guiding light within an air-core confined by a precisely engineered silica glass-air cladding structure [16]. Since then, hollow core fibers have been extensively investigated leading to tremendous performance improvements and the demonstration of attenuation levels comparable to standard single-mode fibers [6, 9, 17–24]. In this regard, the emergence of antiresonant hollow core fibers (AR-HCF) offered unprecedented versatility in terms of tailoring the fiber modal properties and great promise for ultra-low loss light guidance [8, 9, 22–27]. In general, these structures consist of a negative curvature air-core interface, and rely on antiresonant and inhibited coupling as the light guiding mechanism [24, 28–33]. Various AR-HCF structures have been demonstrated, ranging from single resonator rings [18] and conjoined tubes [22] to nested [25] and double nested [8] configurations, spanning from strictly single-mode to multimode designs [19].

A unique feature of hollow core fibers is that light can be guided with a minimal fraction of the field overlapping with the glass structure, increasing the damage threshold and reducing material absorption and nonlinearity. Over the years, there have been numerous efforts on power transmission though hollow core fibers, including photonic bandgap [34] and hypocycloidal-core Kagome type structures [35] with single-mode laser power transmission experiments reaching up to 1.2 kW through 1.5 m of fiber [36]. Recent AR-HCF designs have shown great promise for scaling to extreme high-power single-mode delivery, due to

their strong confinement and large core diameter characteristics. As such, the interest in exploring high-power delivery through AR-HCFs has greatly intensified since the demonstration of 300 W single-mode broadband laser transport at 1 μm through a 7-tube AR-HCF [37]. At the ~1000 W level, there have been a few transmission demonstrations involving broad-linewidth sources through both nested and non-nested AR-HCF designs [27, 38, 39]. Significantly, a recent study by Mulvad et al. [27] successfully delivered 1.1 kW output power over across 1 km of nested antiresonant nodeless fiber (NANF) using a 1080 nm source with a spectral linewidth of approximately 6 nm. However, despite these significant advancements, the transmission of multi-kW powers or high-power narrow-linewidth sources in a single-mode fashion remains out of reach. Additionally, these investigations have highlighted the challenge of maintaining adequate coupling efficiency and preventing failure at the fiber input, requiring optical alignment adjustments during high-power operation.

In this work, we demonstrate transmission of multi-kW narrow-linewidth single-mode power through a 6.25 m long 5-tube NANF. By coupling a 2.3 kW single-mode CW laser operating at 1080 nm, with a beam quality (M^2) of 1.045, we achieved an output power of 2.2 kW at 84 GHz linewidth, while maintaining near diffraction-limited beam quality. We precisely tailor the beam coupled into the hollow core fiber, ensuring exceptional stability and eliminating the need for realignment at high power levels. Furthermore, for laser configurations with linewidths of 64 GHz and 38 GHz, we obtained output powers of 2.17 kW and 1.7 kW, respectively, limited only by the maximum power of the source.

The low-loss NANF used in the experiments was fabricated in-house with attenuation of 0.79 dB/km at 1080 nm. In Fig. 1(a), we present a scanning electron microscope (SEM) image of the NANF facet with core diameter of ~23 μm and thickness of outer tubes and nested tubes of 780 $nm \pm 10$ nm. The attenuation spectrum was obtained via a 463 m cutback measurement, Fig. 1(b). Using the $1/e^2$ definition, the mode field diameter (MFD) was found to be ~18 μm at 1080 nm, which is in excellent agreement with the calculated MFD when simulating the structure shown in Fig. 1(a).

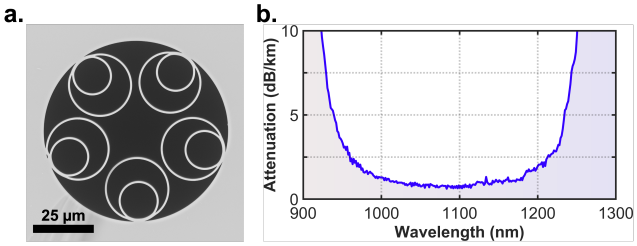

Fig. 1. Characterization of the fabricated NANF fiber. (a) SEM image of the 5-nested tubes NANF. (b) Measured spectral attenuation.

To investigate the power delivery performance of the NANF, we employed a CW fiber laser amplifier system capable of producing up to 2325 W with an 84 GHz linewidth. The laser source utilized a three-stage Yb-doped fiber amplifier architecture and an external seed connected to a phase modulator for spectral broadening. The seed operated at a wavelength of 1080.14 nm and a 1 MHz linewidth. Inline RF attenuators served to control the resulting linewidth of the modulated seed. Figure 2, shows a schematic of the experimental setup.

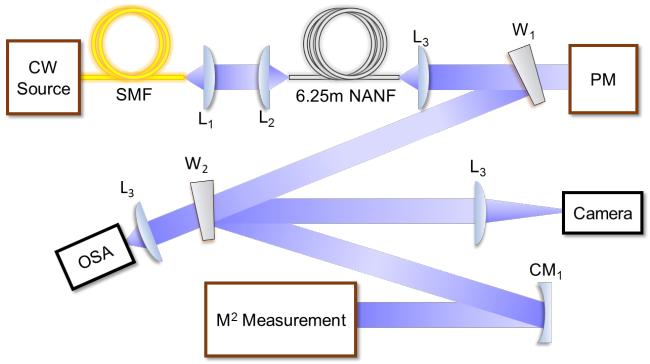

Fig. 2. Schematic of the experimental setup. A high-power CW fiber laser amplifier system is coupled into a 6.25 m long NANF. Large mode area (LMA) fiber; L_1, L_2, L_3, L_4, L_5 plano-convex lenses; W_1 and W_2 fused silica wedges; Power meter (PM); optical spectrum analyzer (OSA); M_1 plano-concave mirror.

The fiber laser output was delivered through a large mode area (LMA) fiber and collimated using a plano-convex lens (L_1). The resulting collimated beam was then free-space coupled to the 5-tube NANF which had a total length of 6.25 m. To match the mode field diameter of the NANF, a second plano-convex lens (L_2) was used, resulting in a numerically calculated coupling efficiency of ~98%. To minimize localized thermal drift and distortion during operation, the fiber was mounted on a custom fixture, and precise alignment between the LMA fiber and the NANF was achieved using 5-axes stages. The NANF was coiled on an uncooled 25 cm diameter grooved aluminum mandrel. For power measurement and monitoring, the output of the NANF was collimated using the same method as the input and directed through an antireflection coated fused-silica wedge (W_1). A low-power reflection from the wedge was fed into the beam diagnostics equipment. Over 99.93% of the fiber output power was captured and measured using a 5 kW power meter (Ophir 5000W-BB-50).

The output beam was characterized by conducting M^2, spectral, and mode profile measurements. To accomplish this, we utilized the first reflection of the low-power pickoff (W_1), which was directed towards an uncoated fused-silica wedge (W_2). The transmitted light through W_2 was then coupled to an optical spectrum analyzer (OSA) with a resolution of 7.5 GHz (Thorlabs BP209-IR2) using a single-mode fiber patch cable. Simultaneously, the front surface reflection from W_2 was directed towards a beam profiler to determine the beam divergence and calculate the M^2 values in the X and Y directions. For imaging purposes, the back surface reflection of W_2 was captured by a CMOS camera through a 400 mm focal length lens (L_5) providing adequate magnification. It is important to note that in our experimental setup, the imaged beam originates from back reflections of W_2, resulting in the beam passing through the wedge material twice. This introduces a slight elliptical distortion at the image plane due to the wedge.

Coupling from the laser LMA fiber to the NANF was performed at low power (below 5W). At this point, we measured a transmission efficiency of 97.3% through the NANF. After we optimized the input coupling conditions at low power, no additional adjustments to the NANF input coupling were performed

for the entire duration of high power testing. Subsequently, we increased the power to about 20 W. This higher power allowed us to align the optical diagnostics components, as illustrated in Fig. 2. After diagnostics alignment at this power level, we gradually increasing the power in ∼220W increments. At each power increment, we allocated a 120-second pause to monitor any potential thermal drift and to ensure that the power meter reached a steady state before recording measurements. The temperature of the fiber was continuously monitored using a handheld thermal camera (FLIR T560). The first evaluation at high power was conducted with an 84 GHz linewidth and subsequently repeated at 64 GHz and 38 GHz linewidths.

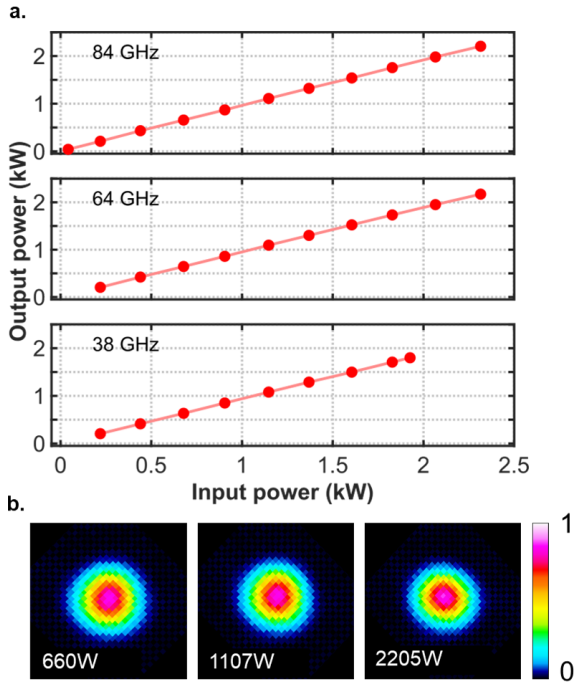

Fig. 3. Experimental narrow-linewidth laser delivery through hollow core fiber. (a) Output power as function of input power for three different source linewidth configurations. (b) Far field beam profiles at the output of the 6.25 m NANF for different transmitted powers at 84 GHz linewidth.

Input Power (W) ±4%	Input M^2 ±5%	Output M^2 ±5%	Transmission Efficiency ±0.5%
219	1.065	1.050	96.4%
678	1.050	1.035	96.8%
1147	1.045	1.035	96.7%
1605	1.045	1.030	96.0%
2066	1.045	1.015	95.9%
2315	1.045	1.020	95.3%

Table 1. Beam quality and transmission efficiency measurements with the single-mode 84 GHz linewidth source

In Fig. 3(a), we present the power transmission results for the three different spectral linewidth conditions. Beam profiles corresponding to 0.5 kW, 1 kW, and 2kW transmission outputs are depicted in Fig. 3(b). The maximum laser power of the source was limited to 2.315 kW for both 84 GHz and 64 GHz, and further limited to 1.828 kW at 38 GHz. Our experimental findings demonstrate successful laser delivery through the NANF, with power values of 2.205 kW, 2.170 kW, and 1.708 kW achieved at 84 GHz, 64 GHz, and 38 GHz, respectively. At maximum power, these results correspond to transmission efficiencies of 95.4%, 94%, and 93.6% for each respective linewidth. The slightly lower efficiencies observed for the latter two cases can be attributed to micrometer scale misalignment of the coupling conditions. The fiber input launching conditions were not re-optimized during the experiments, which emphasizes the stability of the NANF and input coupling optics.

Throughout the study, the temperature at the input interface of the NANF remained below 82°C, while the temperature along the length of the fiber did not exceed 42°C. We collected beam quality measurements at each input power step, and the results for the 84 GHz linewidth case are shown in Table 1, alongside the corresponding transmission efficiency. M^2 is reported as the total M^2 defined as $M^2 = \sqrt{M_x^2 M_y^2}$. We observed a slight decrease in transmission efficiency as the input power was increased, as can be seen in Table 1. This could be attributed to minor alignment drift at the NANF input or slight beam distortions caused by thermal lensing on the coupling optics.

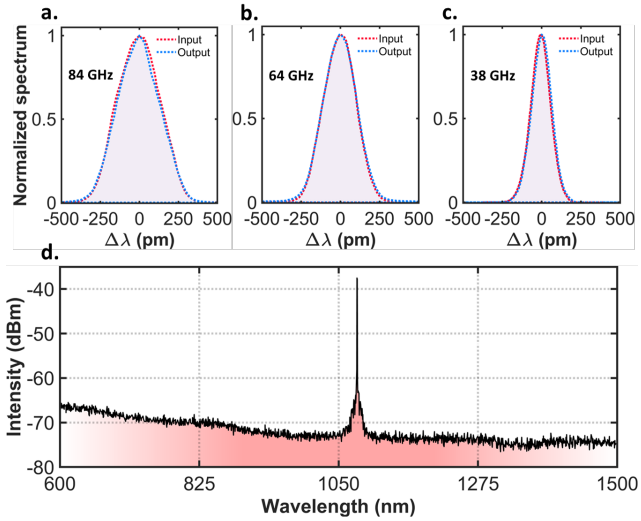

Fig. 4. Spectral characterization of the laser beam. Spectral measurements obtained at maximum power for each source linewidth configuration: (a) 84 GHz, (b) 64 GHz, (c) 38 GHz. Measured input signal spectra from the laser source are depicted in red, while the NANF output spectra are represented in blue. (d) Measured output spectrum covering the spectral wavelength range from 600 nm to 1500 nm for 2.2 kW and 84 GHz transmission.

To gain a better understanding of potential nonlinear distortions in the NANF, we conducted spectral measurements at the maximum transmitted powers for each linewidth configuration, as depicted in Fig. 4. Narrow wavelength scans are shown in Figs. 4(a-c) corresponding to 84 GHz, 64 GHz, 38 GHz inputs, respectively. The central wavelength corresponds to 1080 nm. For each case, the measured input signal spectra from the fiber laser source are depicted in red, while the NANF output spectra

are represented in blue. One can observe that the linewidth of the source is preserved through the fiber. In addition, we performed a wavelength scan covering the spectral range from 600 nm to 1500 nm for 2.2 kW output power at 84 GHz as shown in Fig. 4(d). Under these conditions, the spectrum exhibits only the central peak of the source located near 1080 nm. These measurements confirm that there are no additional spectral features or broadening attributed to nonlinear processes resulting from the high energy densities within the NANF.

In conclusion, we have demonstrated delivery of narrow-linewidth single-mode laser power through a hollow core fiber at a record average power of 2.2 kW. This was enabled by an in-house fabricated low-loss 5-tube NANF, which exhibits a loss of 0.79 dB/km at 1080 nm. We have shown that our NANF can reliably transmit high power levels, achieving output powers of 2.2 kW, 2.17 kW, and 1.7 kW, with spectral linewidths of 84 GHz, 64 GHz, and 38 GHz, respectively. The measured transmission efficiency was above 95% at 2.2 kW. Furthermore, our fiber provides robust single-mode performance with M^2 of 1.045. The NANF effectively mitigates nonlinear effects, as evidenced by the absence of measurable nonlinear distortions in the delivered laser beam. Our results could pave the way for high-brightness narrow-linewidth fiber delivery systems for a wide range of applications.

Funding. This effort was sponsored, in part, by the Army Research Office (W911NF1910426).

Acknowledgments. M.C. acknowledges support from the SPIE, the Directed Energy Professional Society, and the Northrop Grumman graduate scholarship programs. The authors would like to thank David Scerbak from Coherent Corp. for facilitating access to the high-power laser.

Disclosures. The authors declare no conflicts of interest.

Data availability. Data underlying the results presented in this paper are not publicly available at this time but may be obtained from the authors upon reasonable request.

REFERENCES

1. Y. Zhao, J. Zhu, W. He, Y. Liu, X. Sang, and R. Liu, "3d printing of unsupported multi-scale and large-span ceramic via near-infrared assisted direct ink writing," Nat. Commun. **14** (2023).
2. C. Gaida, M. Gebhardt, T. Heuermann, F. Stutzki, C. Jauregui, J. Antonio-Lopez, A. Schülzgen, R. Amezcua-Correa, A. Tünnermann, I. Pupeza *et al.*, "Watt-scale super-octave mid-infrared intrapulse difference frequency generation," Light. Sci. & Appl. **7**, 94 (2018).
3. T. Balciunas, C. Fourcade-Dutin, G. Fan, T. Witting, A. Voronin, A. Zheltikov, F. Gerome, G. Paulus, A. Baltuska, and F. Benabid, "A strong-field driver in the single-cycle regime based on self-compression in a kagome fibre," Nat. communications **6**, 6117 (2015).
4. F. Emaury, C. F. Dutin, C. J. Saraceno, M. Trant, O. H. Heckl, Y. Y. Wang, C. Schriber, F. Gerome, T. Südmeyer, F. Benabid *et al.*, "Beam delivery and pulse compression to sub-50 fs of a modelocked thin-disk laser in a gas-filled kagome-type hc-pcf fiber," Opt. express **21**, 4986–4994 (2013).
5. D. Cruz-Delgado, S. Yerolatsitis, N. K. Fontaine, D. N. Christodoulides, R. Amezcua-Correa, and M. A. Bandres, "Synthesis of ultrafast wavepackets with tailored spatiotemporal properties," Nat. Photonics **16**, 686–691 (2022).
6. F. Poletti, N. V. Wheeler, M. N. Petrovich, N. Baddela, E. Numkam Fokoua, J. R. Hayes, D. R. Gray, Z. Li, R. Slavík, and D. J. Richardson, "Towards high-capacity fibre-optic communications at the speed of light in vacuum," Nat. Photonics **7**, 279–284 (2013).
7. J. R. Hayes, S. R. Sandoghchi, T. D. Bradley, Z. Liu, R. Slavík, M. A. Gouveia, N. V. Wheeler, G. Jasion, Y. Chen, E. N. Fokoua *et al.*, "Antiresonant hollow core fiber with an octave spanning bandwidth for short haul data communications," J. Light. Technol. **35**, 437–442 (2017).
8. G. T. Jasion, H. Sakr, J. R. Hayes, S. R. Sandoghchi, L. Hooper, E. N. Fokoua, A. Saljoghei, H. C. Mulvad, M. Alonso, A. Taranta, T. D. Bradley, I. A. Davidson, Y. Chen, D. J. Richardson, and F. Poletti, "0.174 db/km hollow core double nested antiresonant nodeless fiber (dnanf)," in *Optical Fiber Communication Conference (OFC) 2022*, (Optica Publishing Group, 2022), p. Th4C.7.
9. J. H. Osório, F. Amrani, F. Delahaye, A. Dhaybi, K. Vasko, F. Melli, F. Giovanardi, D. Vandembroucq, G. Tessier, L. Vincetti, and et al., "Hollow-core fibers with reduced surface roughness and ultralow loss in the short-wavelength range," Nat. Commun. **14** (2023).
10. D. J. Richardson, J. Nilsson, and W. A. Clarkson, "High power fiber lasers: current status and future perspectives [invited]," J. Opt. Soc. Am. B **27**, B63–B92 (2010).
11. J. Dai, C. Shen, N. Liu, L. Zhang, H. Li, H. He, F. Li, Y. Li, J. Lv, L. Jiang, Y. Li, H. Lin, J. Wang, F. Jing, and C. Gao, "10 kw-level output power from a tandem- pumped yb-doped aluminophosphosilicate fiber amplifier," Opt. Fiber Technol. **67**, 102738 (2021).
12. S. Du, T. Qi, D. Li, P. Yan, M. Gong, and Q. Xiao, "10 kw fiber amplifier seeded by random fiber laser with suppression of spectral broadening and srs," IEEE Photonics Technol. Lett. **34**, 721–724 (2022).
13. J. W. Dawson, M. J. Messerly, R. J. Beach, M. Y. Shverdin, E. A. Stappaerts, A. K. Sridharan, P. H. Pax, J. E. Heebner, C. W. Siders, and C. Barty, "Analysis of the scalability of diffraction-limited fiber lasers and amplifiers to high average power," Opt. Express **16**, 13240–13266 (2008).
14. C. Jauregui, J. Limpert, and A. Tünnermann, "High-power fibre lasers," Nat. Photonics **7**, 861–867 (2013).
15. M. N. Zervas and C. A. Codemard, "High power fiber lasers: A review," IEEE J. Sel. Top. Quantum Electron. **20**, 219–241 (2014).
16. R. F. Cregan, B. J. Mangan, J. C. Knight, T. A. Birks, P. S. J. Russell, P. J. Roberts, and D. C. Allan, "Single-mode photonic band gap guidance of light in air," Science **285**, 1537–1539 (1999).
17. R. Amezcua-Correa, N. G. R. Broderick, M. N. Petrovich, F. Poletti, and D. J. Richardson, "Optimizing the usable bandwidth and loss through core design in realistic hollow-core photonic bandgap fibers," Opt. Express **14**, 7974–7985 (2006).
18. W. Belardi and J. C. Knight, "Effect of core boundary curvature on the confinement losses of hollow antiresonant fibers," Opt. Express **21**, 21912–21917 (2013).
19. W. Shere, E. N. Fokoua, G. T. Jasion, and F. Poletti, "Designing multi-mode anti-resonant hollow-core fibers for industrial laser power delivery," Opt. Express **30**, 40425–40440 (2022).
20. V. Michaud-Belleau, E. N. Fokoua, T. D. Bradley, J. R. Hayes, Y. Chen, F. Poletti, D. J. Richardson, J. Genest, and R. Slavík, "Backscattering in antiresonant hollow-core fibers: over 40db lower than in standard optical fibers," Optica **8**, 216–219 (2021).
21. M. S. Habib, C. Markos, and R. Amezcua-Correa, "Impact of cladding elements on the loss performance of hollow-core anti-resonant fibers," Opt. Express **29**, 3359–3374 (2021).
22. S.-f. Gao, Y.-y. Wang, W. Ding, D.-l. Jiang, S. Gu, X. Zhang, and P. Wang, "Hollow-core conjoined-tube negative-curvature fibre with ultralow loss," Nat. Commun. **9** (2018).
23. F. Amrani, J. H. Osório, F. Delahaye, F. Giovanardi, L. Vincetti, B. Debord, F. Gérôme, and F. Benabid, "Low-loss single-mode hybrid-lattice hollow-core photonic-crystal fibre," Light. Sci. & Appl. **10** (2021).
24. B. Debord, A. Amsanpally, M. Chafer, A. Baz, M. Maurel, J. M. Blondy, E. Hugonnot, F. Scol, L. Vincetti, F. Gérôme, and F. Benabid, "Ultralow transmission loss in inhibited-coupling guiding hollow fibers," Optica **4**, 209–217 (2017).
25. F. Poletti, "Nested antiresonant nodeless hollow core fiber," Opt. Express **22**, 23807–23828 (2014).
26. H. Sakr, Y. Chen, G. T. Jasion, T. D. Bradley, J. R. Hayes, H. C. Mulvad, I. A. Davidson, E. Numkam Fokoua, and F. Poletti, "Hollow core optical fibres with comparable attenuation to silica fibres between 600 and 1100nm," Nat. Commun. **11** (2020).

27. H. C. Mulvad, S. Abokhamis Mousavi, V. Zuba, L. Xu, H. Sakr, T. D. Bradley, J. R. Hayes, G. T. Jasion, E. Numkam Fokoua, A. Taranta, and et al., "Kilowatt-average-power single-mode laser light transmission over kilometre-scale hollow-core fibre," Nat. Photonics **16**, 448–453 (2022).
28. A. D. Pryamikov, A. S. Biriukov, A. F. Kosolapov, V. G. Plotnichenko, S. L. Semjonov, and E. M. Dianov, "Demonstration of a waveguide regime for a silica hollow - core microstructured optical fiber with a negative curvature of the core boundary in the spectral region > 3.5 μm," Opt. Express **19**, 1441–1448 (2011).
29. C. Wei, R. J. Weiblen, C. R. Menyuk, and J. Hu, "Negative curvature fibers," Adv. Opt. Photon. **9**, 504–561 (2017).
30. M. Zeisberger and M. A. Schmidt, "Analytic model for the complex effective index of the leaky modes of tube-type anti-resonant hollow core fibers," Sci. Reports **7** (2017).
31. X. Huang, S. Yoo, and K. Yong, "Function of second cladding layer in hollow core tube lattice fibers," Sci. Reports **7** (2017).
32. A. V. Gladyshev and I. A. Bufetov, "Hollow-core design provides polarization purity," Nat. Photonics **14**, 468–469 (2020).
33. E. N. Fokoua, S. A. Mousavi, G. T. Jasion, D. J. Richardson, and F. Poletti, "Loss in hollow-core optical fibers: mechanisms, scaling rules, and limits," Adv. Opt. Photon. **15**, 1–85 (2023).
34. D. C. Jones, C. R. Bennett, M. A. Smith, and A. M. Scott, "High-power beam transport through a hollow-core photonic bandgap fiber," Opt. Lett. **39**, 3122–3125 (2014).
35. S. Hädrich, J. Rothhardt, S. Demmler, M. Tschernajew, A. Hoffmann, M. Krebs, A. Liem, O. de Vries, M. Plötner, S. Fabian, T. Schreiber, J. Limpert, and A. Tünnermann, "Scalability of components for kw-level average power few-cycle lasers," Appl. Opt. **55**, 1636–1640 (2016).
36. G. Palma-Vega, F. Beier, F. Stutzki, S. Fabian, T. Schreiber, R. Eberhardt, and A. Tünnermann, "High average power transmission through hollow-core fibers," in *Laser Congress 2018 (ASSL),* (Optica Publishing Group, 2018), p. ATh1A.7.
37. X. Zhu, D. Wu, Y. Wang, F. Yu, Q. Li, Y. Qi, J. Knight, S. Chen, and L. Hu, "Delivery of cw laser power up to 300 watts at 1080nm by an uncooled low-loss anti-resonant hollow-core fiber," Opt. Express **29**, 1492–1501 (2021).
38. M. Cooper, J. Wahlen, S. Wittek, J. C. A. Zacarias, D. C. Delgado, J. M. Mercado, I. Divliansky, J. E. Antonio-Lopez, A. Schülzgen, and R. A. Correa, "600 w single mode cw beam delivery via anti-resonant hollow core fiber," J. Dir. Energy **7** (2022).
39. X. Zhu, F. Yu, D. Wu, S. Chen, Y. Jiang, and L. Hu, "Laser-induced damage of an anti-resonant hollow-core fiber for high-power laser delivery at 1 µm," Opt. Lett. **47**, 3548–3551 (2022).